Efficient separation of 1,3-butadiene from C4 hydrocarbons by flexible metal-organic framework with gate-opening effect

Wang Lu[1], Hongliang Huang[1], Zhu Hejin[1], Chang Yanjiao[1], Guo Xiangyu[1], Yang Fan[1], and Chongli Zhong[1]

[1]Tiangong University

June 13, 2021

Abstract

Efficient and economical separation of 1,3-butadiene (C4H6) from C4 hydrocarbons is imperative yet challenging in industrial separation processes. Herein, a guest-induced flexible Mn-bpdc MOF has been employed to separate C4H6 from C4 hydrocarbons, including n-butene (n-C4H8), iso-butene (iso-C4H8), n-butane (n-C4H10) and iso-butane (iso-C4H10). Significantly, C4H6 can instantaneously induce gate-opening of Mn-bpdc MOF at 0.13 bar and 298 K, thus significant amounts of C4H6 can be adsorbed, while other C4 hydrocarbons cannot induce the gate-opening even at 1 bar. The uptake selectivities of Mn-bpdc MOF for C4H6/n-C4H8 and C4H6/iso-C4H8 are up to 40.0 and 45.0 at 298 K and 1 bar, respectively, both surpassing all the reported adsorbents. In addition, breakthrough experiments verified that C4H6/n-C4H8, C4H6/iso-C4H8, C4H6/n-C4H10 and C4H6/iso-C4H10 mixture can be efficiently separated. More importantly, Mn-bpdc possesses excellent water stability and outstanding regeneration ability for C4H6 separation, making it a new benchmark for C4H6 purification.

Efficient separation of 1,3-butadiene from C4 hydrocarbons by flexible metal-organic framework with gate-opening effect

Lu Wang[1,3], Hongliang Huang[1,2*], Hejin Zhu[1,3], Yanjiao Chang[1,2], Xiangyu Guo[1,2], Fan Yang[1,2], Chongli Zhong[1,2]

1. State Key Laboratory of Separation Membranes and Membrane Processes, Tiangong University, No. 399 Binshui West Road, Xiqing District, Tianjin 300387, P. R. China.

2. School of Chemical Engineering, Tiangong University, No. 399 Binshui West Road, Xiqing District, Tianjin 300387, P. R. China.

3. School of Textile Science and Engineering, Tiangong University, No. 399 Binshui West Road, Xiqing District, Tianjin 300387, P. R. China.

*Corresponding authors:

Hongliang Huang Email:*huanghongliang@tiangong.edu.cn*.

Abstract: Efficient and economical separation of 1,3-butadiene (C_4H_6) from C_4 hydrocarbons is imperative yet challenging in industrial separation processes. Herein, a guest-induced flexible Mn-bpdc MOF has been employed to separate C_4H_6 from C_4hydrocarbons, including n-butene (n-C_4H_8), iso-butene (iso-C_4H_8), n-butane (n-C_4H_{10}) and iso-butane (iso-C_4H_{10}). Significantly, C_4H_6can instantaneously induce gate-opening of Mn-bpdc MOF at 0.13 bar and 298 K, thus significant amounts of C_4H_6 can be adsorbed, while other C_4 hydrocarbons cannot induce the gate-opening even at 1 bar. The uptake selectivities of Mn-bpdc MOF for C_4H_6/n-$C_4H_8$and C_4H_6/iso-$C_4H_8$are up to 40.0 and 45.0 at 298 K and 1 bar, respectively, both surpassing

all the reported adsorbents. In addition, breakthrough experiments verify that C_4H_6/n-C_4H_8, C_4H_6/iso-C_4H_8, C_4H_6/n-$C_4H_{10}$and C_4H_6/iso-C_4H_{10}mixture can be efficiently separated. More importantly, Mn-bpdc possesses excellent water stability and outstanding regeneration ability for C_4H_6 separation, making it a new benchmark for C_4H_6 purification.

Keywords: metal-organic frameworks, gate-opening, 1,3-butadiene, adsorption/gas, gas purification.

Introduction

1,3-Butadiene (C_4H_6) is one of the basic and important raw material for petrochemical industry, which not only can be used in the production of synthetic rubber, but also in the synthesis of synthetic resins and other organic chemical products, such as tetramethylene sulfone, tetrahydrofuran.[1-4]It is mainly obtained from the by-product of vapour cracking of naphtha.[5] However, this process is usually accompanied by the presence of other C_4 components, such as n-butene (n-C_4H_8), iso-butene (iso-C_4H_8), n-butane (n-C_4H_{10}) and iso-butane (iso-C_4H_{10}), which will cause structure transformation of polybutadiene in the preparation of synthetic rubber and affect product quality and even reduce polymerization activity by interrupting the polymerization reaction.[6] Hence, the separation of C_4H_6 from the other C_4hydrocarbons is very imperative. In addition, due to the similar boiling point, molecular size and physical properties of C_4 hydrocarbons, especially for diolefin and mono-olefins,[7] the separation of C_4H_6 from other C_4 hydrocarbons is still remain a particular challenge. At present, the separation of C_4H_6 from other C_4 hydrocarbons is mainly carried out by precise controlled extraction distillation in industry.[8]However, the extraction distillation usually needs high operation temperature (323 K to 393 K) with more than 110 trays of high towers,[9] and consume large amounts of organic solvents. In addition, the polymerization of high reactive C_4H_6 is inevitable at above high temperature distillation process.[10] Therefore, the extraction distillation process is energy intensive and environmental unfriendly process, and it is very important to seek for an efficient and low-cost technology to separate $C_4H_6$from C_4 hydrocarbons.

Among the existing separation technologies, adsorption separation featuring simple operating conditions, energy saving, and high adsorption accuracy has been proved to be a potential separation technology with broad prospects for gas separation.[11-13]As an emerging advanced adsorbent, metal-organic frameworks (MOFs) are attracting more and more attention by virtue of their multifarious structural topologies, precise structural determination and tunability of pore surface functionalities.[14-16] In recent years, MOFs have been widely applied to various separation applications, including CO_2 capture,[17]propane-propylene separation,[18,19] hydrogen storage[20]and so on.[21-25] From the point of view of the adsorption mechanism, the efficient separation of gas mixtures by MOFs adsorbents usually depends on the thermodynamic separation based on interaction force,[26,27]kinetic separation determined by adsorption rate,[28-30]molecular sieving separation[31,32] and gate-opening flexible separation.[33,34] Owing to the similarities of molecular sizes, shapes and properties between C_4H_6 and other C_4 hydrocarbons,[35] the potential separation of C_4H_6 from other C_4 hydrocarbons by MOFs adsorbents is still a challenge. The information about physical and chemical properties of C_4 hydrocarbons are illustrated in Table **S1** . Nowadays, most reported MOF adsorbents used for C_4H_6separation from other C_4 hydrocarbons mainly based on the reinforcing interactions between C_4H_6 and MOF over other C_4 hydrocarbons, however the other C_4hydrocarbons could be simultaneously adsorbed to a certain extent,[36-38] especially for the separation of mono-olefins and diolefin. The co-adsorption separations will cause the low adsorption selectivity and low separation efficiency.[39] As well known, molecular sieving is an ideal efficient separation model and has been well achieved on some olefin/alkane separations.[40] However, since the very similar molecular size of C_4H_6 with other C_4hydrocarbons, the adsorbent that can separate C_4H_6 with other C_4hydrocarbons by complete molecular sieving effect have not been reported up to now. Ingeniously, considering the difference that C_4H_6 has two C=C double bonds, whereas the other C_4 hydrocarbons either have one or none C=C double bond, gate-opening flexible MOF hopefully can be deemed as the prospective candidate for the separation of C_4H_6 to achieve the molecular sieving effect. As a very rare example, Kitagawa et al.[41]reported a flexible SD-65 MOF that can selectively capture C_4H_6 and exclude other C_4 hydrocarbons. However, the gate-opening pressure for C_4H_6 is up to 0.6 bar at 298 K. The high gate-opening pressure is disadvantageous for the actual purification and separation of C_4H_6 and the operating range will

be relatively narrow, especially, it is difficult to achieve efficient separation at practical low partial pressure of C_4H_6.[42] Considering this problem, the ideal MOF with gate-opening effect on C_4H_6/C_4 hydrocarbons separation should not only can sensitively capture C_4H_6 at very low pressure but also can exclude other C_4 hydrocarbons even at 1 bar, to realize efficient separation of C_4H_6 over a wide ranges of operation pressures, especially at low partial pressure of C_4H_6.

Herein, we adopt a guest induced flexible Mn-bpdc MOF with neat one-dimensional channels for the separation of C_4H_6 from other four major C_4 hydrocarbons, including two mono-olefins and two paraffins. The intrinsic flexibility of Mn-bpdc MOF is confirmed by thermal responded variable temperature X-ray diffraction (VT-XRD) and guest-depended structure transformations, while its gate-opening effects on olefins and paraffins are explored by the adsorption isotherms of C_2H_4, C_3H_6, C_2H_6 and C_3H_8. Surprisingly, the single-component adsorption isotherms of C_4 hydrocarbons with Mn-bpdc demonstrates that Mn-bpdc can specifically and sensitively capture C_4H_6 with very low gate-opening pressure and exclude for other C_4 components even to 1 bar, including n-C_4H_8,iso-C_4H_8, n-C_4H_{10} and iso-C_4H_{10}. At the same time, the uptake selectivities of C_4H_6/n-$C_4H_8$and C_4H_6/iso-C_4H_8in Mn-bpdc exceed the overall reported adsorbents. The four column breakthrough experiments of gas mixtures of C_4H_6/n-C_4H_8, C_4H_6/iso-C_4H_8, C_4H_6/n-$C_4H_{10}$and C_4H_6/iso-C_4H_{10}furtherly credibly verify that the efficient dynamic separation effect on Mn-bpdc to separate C_4H_6 from other C_4 components can be achieved. In addition, the Mn-bpdc MOF possesses outstanding water stability, well regeneration and cyclic utilization performance, which comprehensively affirm the great potential of Mn-bpdc adsorbent for the challenging separation of C_4H_6 from other C_4hydrocarbons.

Results and Discussion

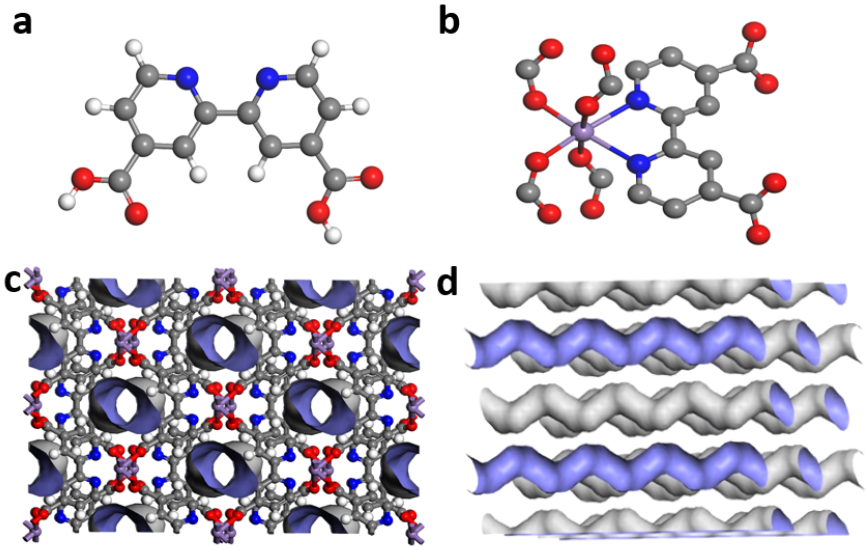

Figure 1. a) 2, 2'-bipyridyl-4, 4'-dicarboxylic acid ligand in Mn-bpdc MOF; **b)** Local coordination geometry of the central Mn metal atoms; **c)** The 3D structure and connolly surface of Mn-bpdc MOF front view of the structure along the c axis; **d)**The one-dimensional channels of Mn-bpdc MOF. The inner and external surfaces are lilac and grey, respectively. Color codes: Grey violet, red, dark blue, and gray nodes represent manganese metal, oxygen, nitrogen and carbon atoms, respectively.

The Mn-bpdc MOF was synthesized by hydrothermal method through the reaction of commercially available 2,2'-bipyridine-4,4'-dicarboxylic acid ligand (H_2BPDC) and manganese sulfate.[43] The experimental PXRD pattern of the as-synthesized Mn-based MOF is accorded with the simulated ones, revealing the successful synthesis of Mn-bpdc MOF (**Figure S1**). The framework of Mn-bpdc consists of infinite chains of corner-sharing Mn(II) centers connected with two nitrogen atoms from bipyridyl and four oxygen atoms from

carboxylic of BPDC ligands, possessing uniform one dimensional channels (**Figure 1a-d**). The scanning electron microscopy (SEM) of Mn-bpdc MOF is showed in **Figure S2,** which reveals that the Mn-bpdc MOF has rod-shaped laminated microstructures.

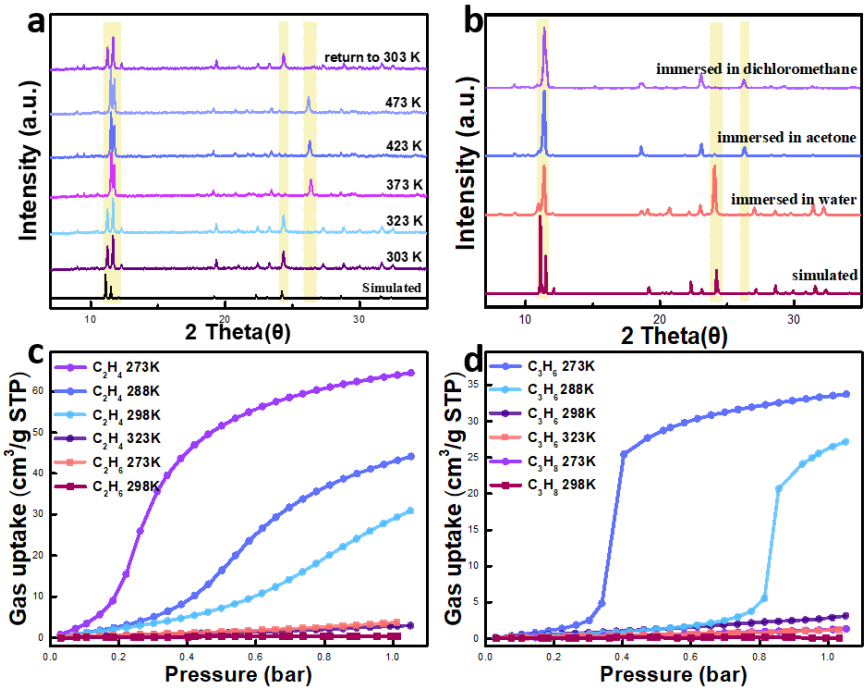

Figure 2. **a)** VT- PXRD patterns of Mn-bpdc MOF at different temperatures under atmospheric environment; **b)** PXRD patterns of Mn-bpdc MOF after different treatments by immersing in acetone, dichloromethane and water, respectively; **c)** Adsorption isotherms of Mn-bpdc MOF for single component$\mathbf{C_2H_4}$ and$\mathbf{C_2H_6}$ at different temperatures;**d)** Adsorption isotherms of Mn-bpdc MOF for single component$\mathbf{C_3H_6}$ **and** $\mathbf{C_3H_8}$ at different temperatures.

To investigate the flexible structure of Mn-bpdc, firstly, the VT-PXRD measurements at different temperatures under atmospheric environment were measured, as drawn in **Figure 2a** . At the temperatures of 303 K and 323 K, the PXRD patterns are consistent with the simulated ones. When the temperature raises from 373 K to 473 K, the diffraction peak at around 11.3° slightly shifts to the high angle, while new diffraction peak appears at 26.3° and the pristine diffraction peaks at 24.1°of Mn-bpdc at 303 K and 323 K completely disappears, which illustrate temperature responded structural transformation of Mn-bpdc. It is worth noting that when the temperature drops from 473 K to 303 K, the PXRD patterns were restored to the original state at 303 K, which indicates that the reversible structure transformation of Mn-bpdc upon thermal stimulation. To explore the guest molecule induced structural transformation of Mn-bpdc, we measured the PXRD of the Mn-bpdc MOF samples by immersing in water, dichloromethane and acetone, respectively. The PXRD pattern of Mn-bpdc under water environment is consistent with that simulated one (**Figure 2b**). However, the PXRD patterns change obviously when the MOF immersed in acetone or dichloromethane, and the diffraction peaks at 24.1° disappear while new diffraction peaks appear at 26.3°, which indicates that guest molecules can also induce the structure transformation of Mn-bpdc. In addition, when the dichloromethane treated Mn-bpdc MOF was exchanged by water, the consistent PXRD pattern of water exchanged Mn-bpdc MOF **(Figure S4)** with simulated ones credibly verifies the structural reversibility of Mn-bpdc MOF. In a word, it illustrates that both thermal stimulation and guest molecule induction can trigger the structural transformation of the Mn-bpdc MOF.

Taking into account the peculiarity of both temperature and guest molecular can induce structural transformation, gas molecules with different polarity might also be able to regulate the structural transformation of the Mn-bpdc MOF at proper temperature. To study the stimulus-response behavior of Mn-bpdc towards gas molecules, the single-component gas adsorption isotherms of $C_2H_4$and C_3H_6were collected at 273 K, 288 K, 298 K and 323 K, respectively, as shown in **Figure 2c** . For the C_2H_4 adsorption at 323K, there is almost no observed adsorption even up to 1 bar, indicating that C_2H_4 cannot open the door of Mn-bpdc at 323 K. However, when the temperature reduces, obvious adsorption begins to be observed at 273 K, which shows typical S-typed curves and implies structural transformation in the adsorption process.[44,45] In particular, the lower adsorption temperatures, the lower gate-opening pressures can be achieved, illustrating that low temperature is more conducive for C_2H_4 to open the door of Mn-bpdc. Similar results also can be observed for C_3H_6 adsorption (**Figure 2d**). We can obviously find that it fails to open the door at both 298 K and 323 K for C_3H_6 adsorption, but the gate-opening effects are appeared at 273 K and 288 K, corresponding to the gate-opening pressure points at 0.35 bar and 0.80 bar, respectively. These results mean that the gate-opening pressure points of adsorption can be well regulated by different temperatures and object gas molecule. In addition, the single component gas sorption isotherms of Mn-bpdc MOF for C_2H_6 (**Figure 2c**) and C_3H_8 (**Figure 2d**) were measured both at 273 K and 298 K. Obviously, no matter at 273 K or 298 K, they have no ability to open the door of Mn-bpdc MOF, which suggests that the occurrence of gate-opening can be induced by the C=C double bond of olefins. Furtherly, compared the adsorption curves of C_2H_4 and C_3H_6 at 273 K, it should be noticed that the gate-opening points of C_2H_4 (0.2 bar) is lower than that of C_3H_6 (0.35 bar). Similar changes of gate-opening pressure can also be observed for C_2H_4 and C_3H_6 adsorption at 298 K. It verifies that C_2H_4 has higher capability to induce the gate-opening behavior of Mn-bpdc than that of C_3H_6, and gate-opening pressure of Mn-bpdc will increase when the number of carbon atoms increased in mono-olefines.

Enlightened by the above experimental results, it implies that Mn-bpdc depending on its structural response to different types olefins can achieve the separation of C_4H_6 from other C_4 at room temperature. In detail, since C_4H_6 has two C=C double bonds, it could be more easily to open the door of Mn-bpdc MOF with lower gate-opening pressure. On the contrary, for other C_4 components, the gate-opening ability will be weaker due to the increases of carbon atoms numbers. Since C_3H_6 cannot open the door of Mn-bpdc even up to 1 bar at 298 K, we can infer that n-C_4H_8 and iso-C_4H_8 will fail to open the door at 298 K although they have one C=C double bond. On the other hand, n-C_4H_{10} and iso-C_4H_{10} also certainly cannot open the gate of Mn-bpdc at 298 K owning to the absence of C=C double bond. Hence, theoretically, the Mn-MOF can efficiently separate C_4H_6 from other C_4hydrocarbons by recognizing C_4H_6 and rejecting other C_4 hydrocarbons to enter the framework of Mn-bpdc MOF at room temperature.

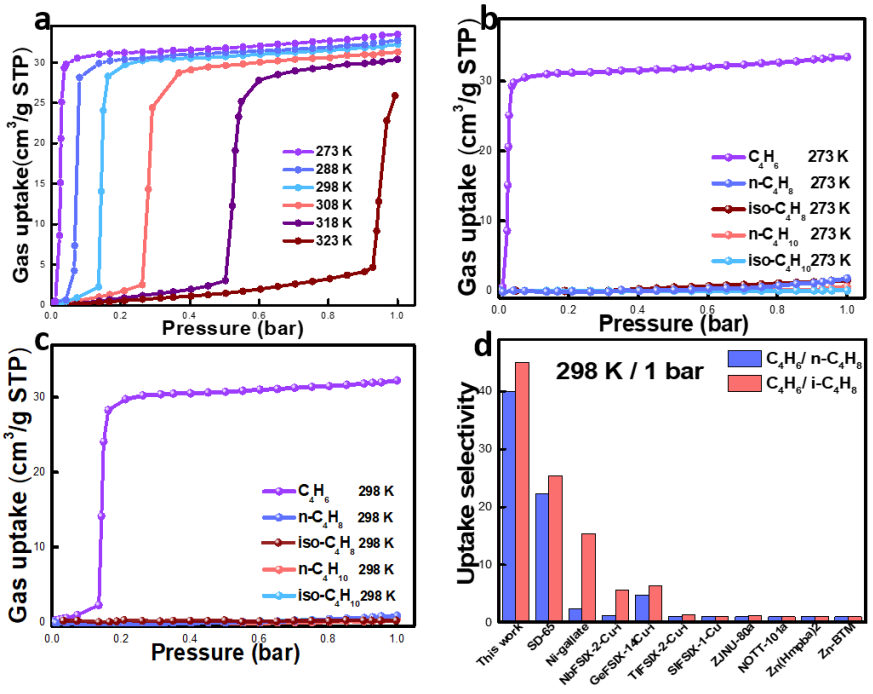

Figure 3. **a)** Adsorption isotherms of Mn-bpdc MOF for single component C_4H_6 at different temperatures;**b)** Adsorption isotherms of Mn-bpdc MOF for single component C_4H_6, n-C_4H_8, iso-C_4H_8, n-C_4H_{10} and iso-C_4H_{10} at 273 K; **c)**Adsorption isotherms of Mn-bpdc MOF for single component C_4H_6, n-C_4H_8, iso-C_4H_8, n-C_4H_{10} and iso-C_4H_{10} at 298 K, respectively;**d)** The comparison of uptake selectivity of C_4H_6/n-$C_4H_8$and C_4H_6/iso-$C_4H_8$with reported adsorbents at 298 K and 1 bar.

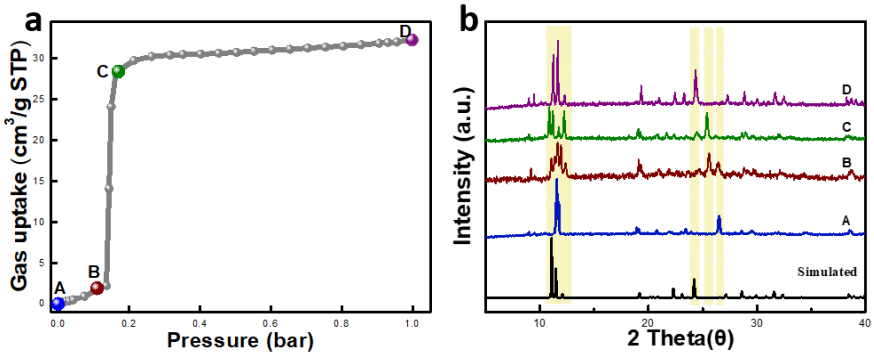

Figure 4. **(a)** Adsorption isotherms of Mn-bpdc marked with four adsorption positions for C_4H_6 at 298 K;**(b)** *In situ* PXRD experiments collected under different gas pressures corresponding to the four adsorption positions as shown in**(a)** , point A (0 bar), point B (0.11 bar), point C (0.17 bar), point D (1 bar).

To confirm our hypothesis, firstly, the adsorption isotherms of C_4H_6 at different temperatures were collected. As shown in **Figure 3a** , the Mn-bpdc MOF exhibits abrupt adsorption phenomenon for C_4H_6 at all temperatures, including 273 K, 288 K, 298 K, 308 K,318 K and 323 K. As expected, the gate-opening pressure for $C_4H_6$is found to be as low as 0.13 bar at 298 K by virtue of the presence of two C=C double bonds. In addition, the C_4H_6uptake at 0.20 bar is about 30 cm^3g^{-1}, 93 % of that at 1 bar (32.12 cm^3 g^{-1}),

which both demonstrates that $C_4H_6$with double C=C bonds has strong ability to open the doors of Mn-bpdc MOF.[46] Besides, the gate-opening pressure is observed to be increased with the increasing of adsorption temperature. In detail, at 273 K, 288 K, 308 K,318 K and 323 K, the abrupt gate-opening pressures are 0.02 bar, 0.06 bar, 0.26 bar, 0.50 bar, 0.92 bar (**Figure S5**), corresponding to the uptake of 33.57 cm^3g^{-1}, 32.81 cm^3g^{-1}, 31.40 cm^3g^{-1}, 30.51 cm^3 $g^{-1}$and 26.04 cm^3 g^{-1} at 1 bar, respectively. Consisting with the observations of C_2H_4 and C_3H_6 adsorptions, it can be found that lower temperatures are more conducive to opening the door of Mn-bpdc for C_4H_6, which dues to the gas molecules slow down at low temperatures and are more likely to be bound by MOF, thus providing adequate gate-opening capacity per unit time.[47,48] In addition, compared with the gate-opening pressures of C_2H_4 (nearly 1 bar) and C_3H_6 (cannot open the gate even at 1 bar) at 298 K, C_4H_6 can open the flexible door of Mn-bpdc MOF at very low pressure (0.13 bar) (**Figure S5**), which is consistent with the previous inferences. It should be noticed that although the SD-65 MOF with gate-opening effect has been reported for C_4H_6separation from other C_4 mono-olefines and paraffins, the gate-opening pressure of SD-65 reaches up to 0.6 bar at 298 K.[41] Obviously, the very low gate-opening pressure of Mn-bpdc for $C_4H_6$is a huge advantageous to achieve efficient separation of $C_4H_6$from other C_4 hydrocarbons at lower partial pressure of C_4H_6.

Subsequently, the adsorption isotherms for n-C_4H_8, iso-C_4H_8, n-C_4H_{10} and iso-C_4H_{10} were measured at 273 K (**Figure 3b**) and 298 K (**Figure 3c**), respectively. At 273 K and 1 bar, there are almost no uptakes for n-C_4H_8 (1.78 cm^3g^{-1}), iso-C_4H_8 (1.48 cm^3 g^{-1}), n-C_4H_{10} (0.61 cm^3g^{-1}) and iso-C_4H_{10}(0.05 cm^3 g^{-1}), but high uptake for C_4H_6 (34.12 cm^3g^{-1}) is retained. Additionally, the uptake of C_4H_6 at the gate-opening pressure of 0.02 bar is closed to the maximum adsorption capacity. The distinct difference between adsorption isotherms of C_4H_6 and other C_4hydrocarbons means great theoretical selectivity could be achieved and this MOF has huge potential for actual separation of C_4H_6 over other C_4hydrocarbons. Importantly, the very low uptakes of n-C_4H_8 (0.80 cm^3g^{-1}), iso-C_4H_8 (0.74 cm^3 g^{-1}), n-C_4H_{10} (0.29 cm^3g^{-1}) and iso-C_4H_{10}(0.02 cm^3g^{-1}) can be also observed at 298 K and 1 bar. The extreme low uptakes illustrate that the Mn-bpdc MOF is very negative to capture n-C_4H_8, iso-C_4H_8, n-C_4H_{10} and iso-C_4H_{10}. On the contrary, by virtue of much stronger polarity of C_4H_6, it can actively push open the molecular door of Mn-bpdc MOF, which is definitely verified by the very low gate-opening pressure (0.13 bar) and close saturation adsorption capacity of C_4H_6 (32.2 cm^3g^{-1}) at the low pressure. As we known, the adsorption selectivity is a critical factor to evaluate the separation performance for adsorbent materials.[49] Notably, the calculated uptake selectivities of Mn-bpdc MOF for C_4H_6/n-$C_4H_8$and C_4H_6/iso-$C_4H_8$are 40.0 and 45.0 at 298 K and 1 bar, respectively, both of which are much higher than that all previous porous materials. (Mg-gallate: 1.3, 15.1;[50] Ni-gallate: 2.4, 15.4;[50]GeFSIX-14-Cu-i: 4.7, 6.4;[37] NbFSIX-2-Cu-i: 1.2, 5.7;[37] GeFSIX-2-Cu-i: 1.1, 2.9;[37]ZJNU-30a: 1.0, 1.2;[36] and SD-65: 22.3, 25.4;[41] **Figure 3d** and **Table S2**). Those results powerfully indicate the potential utility of Mn-bpdc MOF for the separation of C_4H_6 from other C_4 hydrocarbons under ambient conditions.

Furtherly, to explore the structure variations upon the adsorption of C_4H_6 and directly observe the guest-induced structural transformations, we measured the *in situ*PXRD of Mn-bpdc under C_4H_6 environment with different pressures (0 bar, 0.11 bar, 0.17 bar and 1 bar) at 298 K (**Figure 4b**). The four different pressures points at *in situ* PXRD data are corresponded to the detailed adsorption points in the adsorption curves of C_4H_6 at 298 K (Figure 4a). As shown in **Figure 4b** , compared with the PXRD pattern of Mn-bpdc under vacuum environment (point A), obvious new diffraction peak at 25.4° appears and slight peak at 24.4° begins to appear when the pressure increases to 0.11 bar (point B), which means small amount adsorption of C_4H_6 before isotherm obviously jumping can lead to the initial transformation of the structure of Mn-bpdc MOF and proves the sensitivity of the structure for C_4H_6. Subsequently, the diffraction peak at 26.5° completely disappears and the peak at 24.4° gradually increases when the pressure raises to 0.17 bar (point C), which corresponds to a large amount of C_4H_6 (28.4 cm^3 g^{-1}) enter the pore structure and furtherly facilitate the structural changes. Then, when the pressure reaches 1 bar and the amount adsorption of C_4H_6 reaches the saturated state, the diffraction peak at 25.4° disappears and the intensity of diffraction peak at 24.4° reaches its maximum value (point D). These results together reveal gradual transformation of the structure of Mn-bpdc in the adsorption process of C_4H_6. In addition, it is found that the strong peaks at around 11.6° under vacuum transforms into several unidentifiable weaker diffraction peaks when

the pressures increased to 0.11 bar and 0.17 bar, then, furtherly splits into two strong peaks at around 11° at 1 bar, which due to the formation of metastable distorted structure of Mn-bpdc at the adsorption process of C_4H_6 and also verifies the huge structure transformation of Mn-bpdc induced by C_4H_6.[41,51] Furtherly, the PXRD pattern of Mn-bpdc after C_4H_6desorption is highly consistent with that of initial vacuum state, which means the well reversibility of structure transformation for C_4H_6 adsorption (**Figure S6**).

Figure 5. Column breakthrough experiment for C_4H_6/n-C_4H_8(1/1 (v/v)) **(a)** ; C_4H_6/iso-C_4H_8(1/1 (v/v)) **(b)** , C_4H_6/n-C_4H_{10}(1/1 (v/v)) **(c)** , C_4H_6/iso-C_4H_{10}(1/1 (v/v)) **(d)** at 298 K, respectively.

To explore the actual separation performance, dynamic fixed-bed column breakthrough experiments were conducted by using binary gas mixtures of C_4H_6/n-C_4H_8(1:1 v/v), C_4H_6/iso-C_4H_8(1:1 v/v), C_4H_6/n-C_4H_{10}(1:1 v/v) and C_4H_6/iso-C_4H_{10}(1:1 v/v) at 298 K, respectively. As shown in **Figure 5(a-d)** , the n-C_4H_8, iso-C_4H_8, n-C_4H_{10} and iso-C_4H_{10} all begin to break through the bed gradually as soon as the feeding of target gas mixture, meanwhile, C_4H_6 keeps continuous adsorption with breakthrough retention times of 167.1 s, 171.8 s, 175.7 s, 177.4 s, respectively, which attributes to its super sensitive gate-opening effect on $C_4H_6$and unrecognized responses for n-C_4H_8, iso-C_4H_8, n-C_4H_{10} and iso-C_4H_{10}. In consequence, the excellent dynamic separation performance toward C_4H_6 for all the binary C_4H_6/n-C_4H_8, C_4H_6/iso-C_4H_8, C_4H_6/n-$C_4H_{10}$and C_4H_6/iso-C_4H_{10}gas mixtures furtherly verifies that this MOF is a very promising soft MOF adsorbent for C_4H_6 purification.

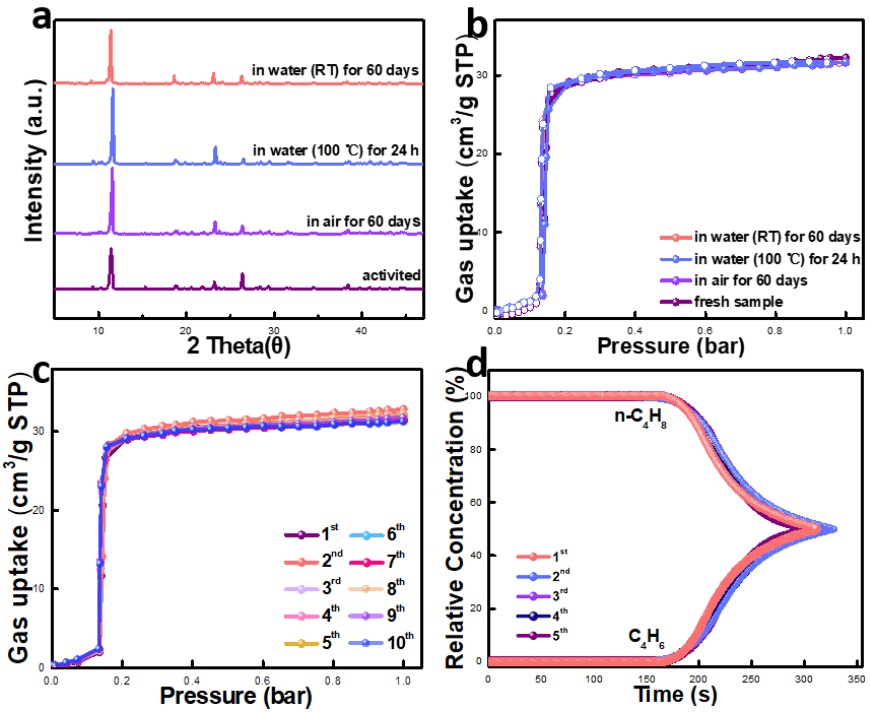

Figure 6. a) PXRD patterns of Mn-bpdc MOF after different treatments by immersing in water (RT) for 60 days, boiled water (100) for 24 hours and air for 60 days, respectively; **b)** Adsorption isotherms of single component C_4H_6 at 298 K for Mn-bpdc samples after different treatments;**c)** Adsorption isotherms of single component C_4H_6 for 10 cycles at 298 K. Adsorption and desorption profiles are shown in closed and open symbols, respectively; **d)** Cycling breakthrough tests for C_4H_6/n-C_4H_8(1/1 (v/v)) separation with Mn-bpdc MOF at 298 K for five times. The column was reactivated with a helium flow at 100 after each breakthrough test.

The excellent stability and regeneration of absorbents are prerequisites for the practical applications in the adsorptive separation of C_4H_6 from C_4hydrocarbons.[52] In order to examine the water stability of Mn-bpdc MOF, we carried out stability tests of Mn-bpdc at water (RT) for 60 days, air for 60 days and boiled water (100) for 24 h. As shown in **Figure 6a** , the PXRD patterns verifies that the framework of Mn-bpdc MOF can well maintain even in those harsh conditions. Furtherly, the C_4H_6 sorption isotherms of Mn-bpdc MOF after different stability tests are shown in**Figure 6b** . The almost identical adsorption isotherms with original simple demonstrate that it can still preserve its intact structure without phase transition and framework collapse after stability treatments.[53]In addition, thermogravimetric analysis (TGA) was performed on the Mn-bpdc MOF to survey its thermal stability. As shown in **Figure S3** , Mn-bpdc MOF can undergo a sustaining 4 % loss of weight up to 360 °C, which dues to the loss of all free molecules. Then, the weight remains constant until the framework begins to collapse at 480 °C. The excellent water and thermal stability of Mn-bpdc MOF can be attributed to the strong coordinate bonds with high coordination numbers formed between central hard acids (Mn^{2+}) and connected four hard bases (CH_3COO^-) and two hard-medial bases (C_5H_5N).[54] The regeneration ability of Mn-bpdc MOF was firstly evaluated by cycling single component adsorption of C_4H_6 at 298 K for ten times. As shown in **Figure 6c** , all the adsorption curves at each cycle are almost consistent and the uptake capacities do not have any loss. Notably, the sample only needs regenerate by vacuum treatment at room temperature instead of degassing by high temperature before each cycle. Furtherly, the PXRD pattern of Mn-bpdc MOF after ten times cycles was measured (**Figure S7)** , which is consistent with activated MOF. In addition, the recycling breakthrough test of Mn-bpdc for C_4H_6/n-C_4H_8separation is shown in **Figure 6d** and the breakthrough times for C_4H_6 remain nearly unchanged after five cycles. Those results comprehensively reveal that the integrality of frameworks can be retained after repeated uses and the Mn-bpdc MOF possesses outstanding recyclability for C_4H_6 adsorption and separation. Importantly, it is a scarce report that confirms Mn-bpdc can be well recycled many times by easily regenerating under vacuum with room temperature and the cost of regeneration will be relatively low. Hence, the excellent water-stability and cycling tests furtherly manifest that it is a great valuable adsorbent for industrial C_4H_6 purification.

Conclusions

In this work, we have employed a flexible Mn-bpdc MOF featuring distinct gate-opening and reversible switch behavior for C_4H_6 purification. The intrinsic flexibility is confirmed by VT-XRD with gradient temperature control. In addition, the different polarity guest-depended molecule can lead to structure transformation with different gate-opening pressure points at different temperatures, such as C_2H_4 and C_3H_6. Importantly, it exhibits prominent gate-opening and abrupt adsorption for C_4H_6 at very low pressure (0.13 bar) but no stimulus-response behavior for all n-C_4H_8,iso-C_4H_8, n-C_4H_{10} and iso-C_4H_{10} even at 1 bar and ambient conditions. Notably, the uptake selectivities of Mn-bpdc MOF for both C_4H_6/n-$C_4H_8$and C_4H_6/iso-C_4H_8surpass whole the reported adsorbents. Furtherly, four dynamic breakthrough experiment results of C_4H_6/n-C_4H_8, C_4H_6/iso-C_4H_8, C_4H_6/n-$C_4H_{10}$and C_4H_6/iso-C_4H_{10}mixtures verifies that this Mn-bpdc MOF can practically separate C_4H_6 from other C_4paraffins and mono-olefins. In addition, the unexpected water stability, benign regeneration ability, signifies that this MOF has great potentiality for industrial C_4H_6 purification and makes it a new benchmark of flexible adsorbent for the separation of C_4H_6 over other C_4hydrocarbons.

Acknowledgements

This work was supported by the National Natural Science Foundation of China (No. 22038010, 21878229, and 21978212), National Key Projects for Fundamental Research and Development of China (No. 2016YFB0600901), and the Science and Technology Plans of Tianjin (19PTSYJC00020 and 20ZYJDJC00110) and we would like to thank the Analytical & Testing Center of Tiangong University for *in situ* XRD measurements.

References

1. Wang H, Liu Y, Li J. Designer metal-organic frameworks for size-exclusion-based hydrocarbon separations: progress and challenges.*Adv Mater.* 2020;32(44):e2002603.

2. Qi L, Zhang Y, Conrad MA, Russell CK, Miller J, Bell AT. Ethanol conversion to butadiene over isolated zinc and yttrium sites grafted onto dealuminated beta zeolite. *J Am Chem Soc* . 2020;142(34):14674-14687.

3. Larina OV, Shcherban ND, Kyriienko PI, et al. Design of effective catalysts based on ZnLaZrSi oxide systems for obtaining 1,3-butadiene from aqueous ethanol. *ACS Sustain Chem Eng* . 2020;8(44):16600-16611.

4. Ul Haq I, Hui Li S, Zhen H-G, Khan R, Zhang A-S, Zhao Z-P. Highly efficient separation of 1,3-butadiene from nitrogen mixture by adsorption on highly stable MOF. *Chem Eng J* . 2020;402:125980.

5. Alves JA, Bressa SP, Martínez OM, Barreto GF. Kinetic evaluation of the set of reactions in the selective hydrogenation of 1-butyne and 1,3-butadiene in presence of n-butenes. *Ind Eng Chem Res* . 2013;52(17):5849-5861.

6. Shirazi SA, Abdollahipoor B, Windom B, Reardon KF, Foust TD. Effects of blending C3-C4 alcohols on motor gasoline properties and performance of spark ignition engines: A review. *Fuel Process Technol* . 2020;197:106194.

7. Mantingh J, Kiss AA. Enhanced process for energy efficient extraction of 1,3-butadiene from a crude C4 cut. *Sep Purif Technol.* 2021;267:118656.

8. Mahdi HI, Muraza O. An exciting opportunity for zeolite adsorbent design in separation of C4 olefins through adsorptive separation. *Sep Purif Technol.* 2019;221:126-151.

9. White WC. Butadiene production process overview. *Chem Biol Interact* . 2007;166(1-3):10-14.

10. Xu W, Hussain A, Liu Y. A review on modification methods of adsorbents for elemental mercury from flue gas. *Chem Eng J* . 2018;346:692-711.

11. Pullumbi P, Brandani F, Brandani S. Gas separation by adsorption: technological drivers and opportunities for improvement. *Curr Opin Chem Eng* . 2019;24:131-142.

12. Chuah CY, Lee Y, Bae T-H. Potential of adsorbents and membranes for SF_6 capture and recovery: A review. *Chem Eng J* . 2021;404:126577.

13. Thompson JA. Acid gas adsorption on zeolite SSZ-13: equilibrium and dynamic behavior for natural gas applications. *AIChE J* . 2020;66(10):e16549.

14. Choi S, Kim T, Ji H, Lee HJ, Oh M. Isotropic and anisotropic growth of metal-organic framework (MOF) on MOF: logical inference on MOF structure based on growth behavior and morphological feature. *J Am Chem Soc* . 2016;138(43):14434-14440.

15. Tang H, Jiang J. In silico screening and design strategies of ethane-selective metal-organic frameworks for ethane/ethylene separation. *AIChE J.* 2020;67(3):e17025.

16. Gao C, Wang P, Wang Z, Kær SK, Zhang Y, Yue Y. The disordering-enhanced performances of the Al-MOF/graphene composite anodes for lithium ion batteries. Nano Energy. 2019;65:104032.

17. Chang Y-J, Huang H-L, Wang L, Li Y, Zhong C-L. Synergistic dual-Li^+ sites for CO_2 separation in metal-organic framework composites. *Chem Eng J* . 2020;402:126201.

18. Abedini H, Shariati A, Khosravi-Nikou MR. Separation of propane/propylene mixture using MIL-101(Cr) loaded with cuprous oxide nanoparticles: Adsorption equilibria and kinetics study. *Chem. Eng. J.* 2020;387:124172.

19. Tan Q, Huang H-L, Peng Y, et al. A temperature-responsive smart molecular gate in a metal-organic framework for task-specific gas separation. *J Mater Chem A* . 2019;7(46):26574-26579.

20. Kapelewski MT, Runcevski T, Tarver JD, et al. Record high hydrogen storage capacity in the metal-organic framework Ni_2(m-dobdc) at near-ambient temperatures. *Chem Mater.* 2018;30(22).

21. Wang L, Huang H-L, Chang Y-J, Zhong C-L. Integrated high water affinity and size exclusion effect on robust Cu-based metal-organic framework for efficient ethanol-water separation. *ACS Sustain Chem Eng* . 2021;9(8):3195-3202.

22. Mi J, Liu F, Chen W, et al. Design of efficient, hierarchical porous polymers endowed with tunable structural base sites for direct catalytic elimination of COS and H_2S. *ACS Appl Mater Interfaces* . 2019;11(33):29950-29959.

23. Das S, Xu S, Ben T, Qiu S. Chiral recognition and separation by chirality-enriched metal-organic frameworks. *Angew Chem Int Ed* . 2018;57(28):8629-8633.

24. Yu G, Liu Y, Zou X, Zhao N, Rong H, Zhu G. A nanosized metal-organic framework with small pores for kinetic xenon separation. *J Mater Chem A* . 2018;6(25):11797-11803.

25. Maes M, Alaerts L, Vermoortele F, et al. Separation of C(5)-hydrocarbons on microporous materials: complementary performance of MOFs and zeolites. *J Am Chem Soc* . 2010;132(7):2284-2292.

26. Lennox MJ, Düren T. Understanding the kinetic and thermodynamic origins of xylene separation in UiO-66(Zr) via molecular simulation.*J Phys Chem C* . 2016;120(33):18651-18658.

27. Ullah S, Bustam MA, Assiri MA, et al. Synthesis and characterization of mesoporous MOF UMCM-1 for CO_2/CH_4adsorption; an experimental, isotherm modeling and thermodynamic study.*Micropor. Mesopor. Mat.* 2020;294:109844.

28. Pimentel BR, Lively RP. Propylene enrichment via kinetic vacuum pressure swing adsorption using ZIF-8 fiber sorbents. *ACS Appl. Mater. Inter.* 2018;10(42):36323-36331.

29. Lyndon R, You W, Ma Y, et al. Tuning the structures of metal-organic frameworks via a mixed-linker strategy for ethylene/ethane kinetic separation. *Chem. Mater.* 2020;32(9):3715-3722.

30. Lee CY, Bae YS, Jeong NC, et al. Kinetic separation of propene and propane in metal-organic frameworks: controlling diffusion rates in plate-shaped crystals via tuning of pore apertures and crystallite aspect ratios. *J Am Chem Soc* . 2011;133(14):5228-5231.

31. Hong X-J, Wei Q, Cai Y-P, et al. Pillar-layered metal-organic framework with sieving effect and pore space partition for effective separation of mixed gas C_2H_2/C_2H_4.*ACS Appl Mater Interfaces* . 2017;9(34):29374-29379.

32. Chen B-L, Zhao X-B, Putkham A, et al. Surface interactions and quantum kinetic molecular sieving for H_2 and D_2 adsorption on a mixed metalorganic framework material. *J Am Chem Soc* . 2008;130:6411-6423.

33. Wang X, Krishna R, Li L, et al. Guest-dependent pressure induced gate-opening effect enables effective separation of propene and propane in a flexible MOF. *Chem Eng J.* 2018;346:489-496.

34. Yang H-Y, Li Y-Z, Jiang C-Y, et al. An interpenetrated pillar-layered metal-organic framework with novel clusters: reversible structural transformation and selective gate-opening adsorption. Cryst Growth Des. 2018;18(5):3044-3050.

35. Assen AH, Virdis T, De Moor W, et al. Kinetic separation of C4 olefins using Y-fum-fcu-MOF with ultra-fine-tuned aperture size.*Chem Eng J.* 2021;413:127388.

36. Luna-Triguero A, Vicent-Luna JM, Poursaeidesfahani A, et al. Improving olefin purification using metal organic frameworks with open metal sites. *ACS Appl Mater Interfaces* . 2018;10(19):16911-16917.

37. Zhang Z, Yang Q, Cui X, et al. Sorting of C4 olefins with interpenetrated hybrid ultramicroporous materials by combining molecular recognition and size-sieving. *Angew Chem Int Ed* . 2017;56(51):16282-16287.

38. Liu H, He Y, Jiao J, et al. A porous zirconium-based metal-organic framework with the potential for the separation of butene isomers.*Chemistry* . 2016;22(42):14988-14997.

39. Liao P-Q, Huang N-Y, Zhang W-X, et al. Controlling guest conformation for efficient purification of butadiene.*Science* . 2017;356:1193-1196.

40. Dey A, Chand S, Maity B, et al. Adsorptive molecular sieving of styrene over ethylbenzene by trianglimine crystals. *J Am Chem Soc.* 2021;143(11):4090-4094.

41. Kishida K, Okumura Y, Watanabe Y, et al. Recognition of 1,3-butadiene by a porous coordination polymer. *Angew Chem Int Ed.* 2016;55(44):13784-13788.

42. Foo ML, Matsuda R, Hijikata Y, et al. An adsorbate discriminatory gate effect in a flexible porous coordination polymer for selective adsorption of CO_2 over C_2H_2. *J Am Chem Soc.*2016;138:3022-3030.

43. Zuo Y, Fang M, Xiong G, et al. Structural diversity, luminescence, and magnetic property: series of coordination polymers with 2,2'-bipyridyl-4,4'-dicarboxylic acid. Cryst Growth Des. 2012;12(8):3917-3926.

44. Li L, Wang Y, Yang J, Wang X, Li J. Targeted capture and pressure/temperature-responsive separation in flexible metal-organic frameworks. *J Mater Chem A.* 2015;3(45):22574-22583.

45. Seo J, Matsuda R, Sakamoto H, et al. A pillared-layer coordination polymer with a rotatable pillar acting as a molecular gate for guest molecules. *J Am Chem Soc* . 2009;131:12792-12800.

46. Wang Z, Sikdar N, Wang S-Q, et al. Soft porous crystal based upon organic cages that exhibit guest-induced breathing and selective gas separation. *J Am Chem Soc* . 2019;141(23):9408-9414.

47. Jin H, Li Y. Flexibility of metal-organic frameworks for separations: utilization, suppression and regulation. *Curr Opin Chem Eng.* 2018;20:107-113.

48. Russell B, Villaroel J, Sapag K, Migone AD. O_2adsorption on ZIF-8: temperature dependence of the gate-opening transition. *J Phys Chem C.* 2014;118(49):28603-28608.

49. Zhang L, Jiang K, Zhang J, et al. A low-cost and high-performance microporous metal-organic framework for separation of acetylene from carbon dioxide. *ACS Sustain Chem Eng* . 2019;7:1667-1672.

50. Chen J, Wang J, Guo L, et al. Adsorptive separation of geometric isomers of 2-butene on gallate-based metal-organic frameworks. *ACS Appl Mater Interfaces* . 2020;12(8):9609-9616.

51. Ye Z-M, Zhang X-W, Liao P-Q, et al. A hydrogen-bonded yet hydrophobic porous molecular crystal for molecular-sieving-like separation of butane and isobutane. *Angew Chem Int Ed* . 2020;59(51):23322-23328.

52. Li H, Li L, Lin R-B, et al. Porous metal-organic frameworks for gas storage and separation: Status and challenges. *J Energy Chem.*2019;1(1):100006.

53. Logan MW, Adamson JD, Le D, Uribe-Romo FJ. Structural stability of N-Alkyl-functionalized titanium metal-organic frameworks in aqueous and humid environments. *ACS Appl Mater Interfaces* . 2017;9(51):44529-44533.

54. Ho TL. Hard soft acids bases (HSAB) principle and organic chemistry.*Chem Rev.* 1975;75(1):1-20.